

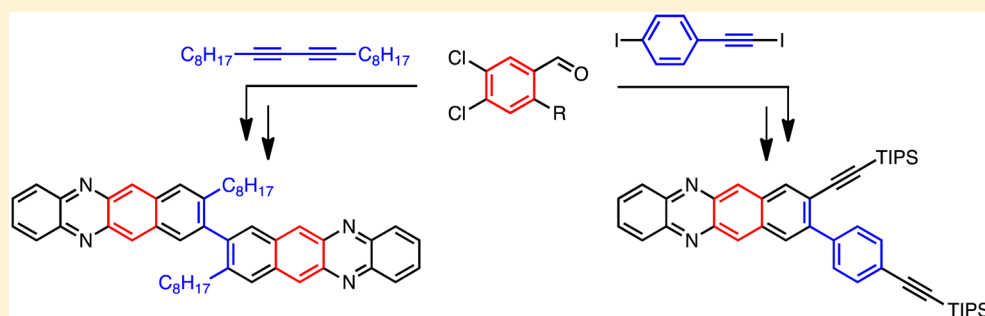
# Diazatetracenes Derived from the Benzannulation of Acetylenes: Electronic Tuning via Substituent Effects and External Stimuli

Dan Lehnher,† Joaquin M. Alzola,†,‡ Catherine R. Mulzer,†,‡ Samuel J. Hein,†,‡ and William R. Dichtel\*,†,‡,§

†Department of Chemistry and Chemical Biology, Baker Laboratory, Cornell University, Ithaca, New York 14853, United States

‡Department of Chemistry, Northwestern University, Evanston, Illinois 60208, United States

§ Supporting Information



**ABSTRACT:** Functionalized diazatetracenes are prepared using a new two-step sequence. The use of a dichlorobenzaldehyde in a Cu-catalyzed benzannulation of acetylenes provides functionalized dichloronaphthalenes that afford diazatetracenes using Buchwald–Hartwig aminations. This approach provides unique substitution patterns and rapid access to covalently linked dimeric diazatetracenes. Their electronic properties are characterized by UV–vis absorption/emission and cyclic voltammetry, revealing strong effects from both external stimuli by acid and internal substituent effects.

## INTRODUCTION

Polycyclic aromatic hydrocarbons (PAHs), such as tetracene and pentacene, and their derivatives have enabled key discoveries and major advances in organic electronics.<sup>1</sup> Polycyclic heteroaromatics, such as those with thiophenes or furans fused to or replacing benzene rings, are of current interest. Desirable optoelectronic properties emerge or are enhanced in structures that incorporate sulfur,<sup>2</sup> oxygen,<sup>3</sup> boron,<sup>4</sup> and nitrogen<sup>5</sup> and are potentially relevant for sensing, lighting, charge transport, energy conversion, and energy storage.<sup>6</sup> Miao and Bunz reported N-heteroacenes, such as heteroacenes of pentacenes,<sup>5a–c</sup> which behave as n-type semiconductors and sometimes exhibit ambipolar charge transport.<sup>5a–c</sup> Nitrogen incorporation can enhance the rate of singlet fission,<sup>7</sup> in which two triplet excited states are generated from the absorption of a single photon, which is of interest for third-generation photovoltaic materials.<sup>8</sup> Therefore, synthetic methods that open new avenues to access N-heteroacenes and tune their properties are of significant interest. We recently reported a regioselective synthesis of polyhalogenated naphthalenes via the benzannulation of haloalkynes.<sup>9–11</sup> Here, we leverage this powerful method to access functionalized, solution-processable diazatetracenes (formally known as benzo-[b]phenazines). Herein, we report their expedient synthesis and the ability to tune their electronic properties via either external stimuli or substituent choice.

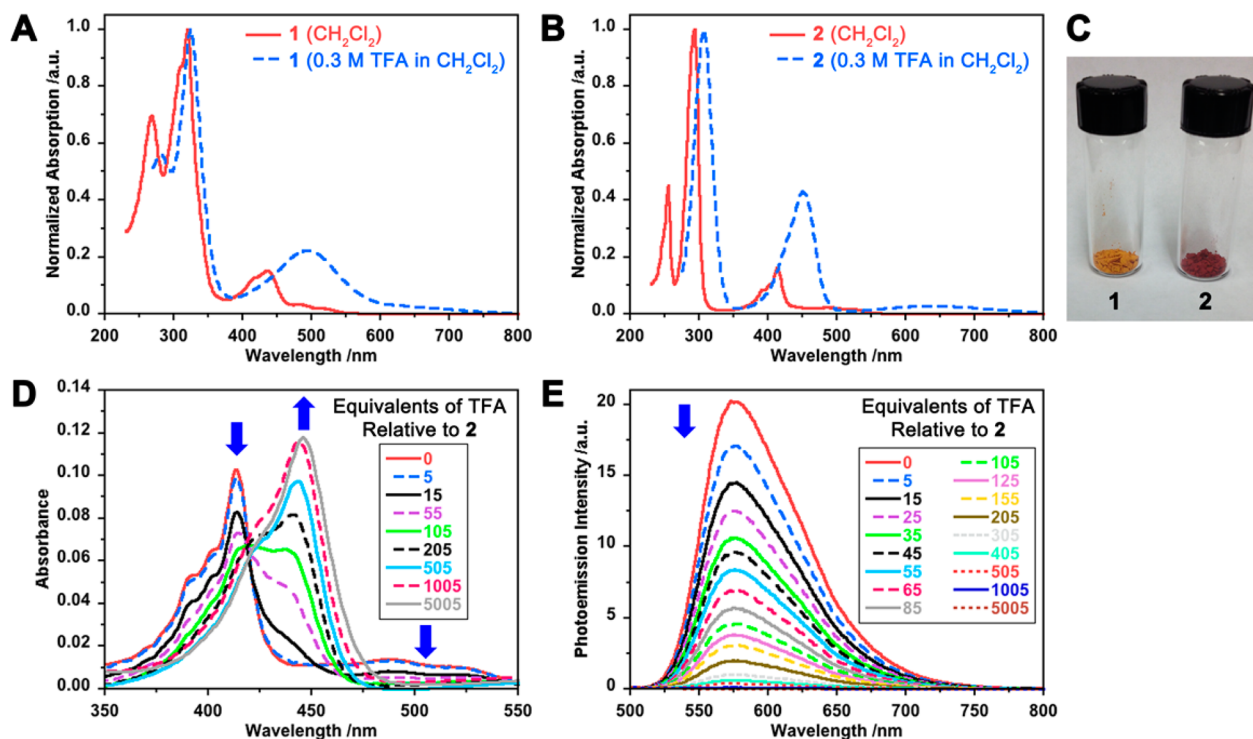
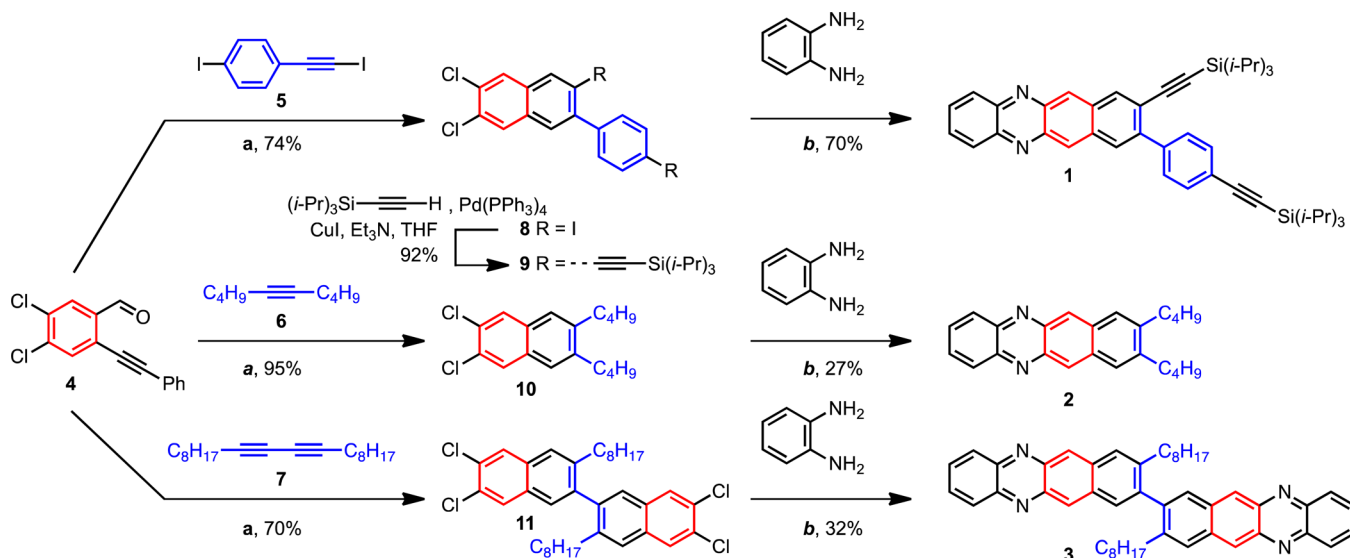
## RESULTS AND DISCUSSION

Diazatetracenes **1–3** were synthesized using a two-step procedure (Scheme 1): (1) assemble a dichloronaphthalene via a Cu-catalyzed benzannulation of an alkyne using dichlorobenzaldehyde **4** and then (2) subject the dichloronaphthalene to a Buchwald–Hartwig amination with 1,2-diaminobenzene to form the diazatetracene core with concomitant aromatization. Cu-catalyzed benzannulation of aryl haloalkyne **5**, dialkylacetylene **6**, and dialkyl diyne **7** proceed to the desired functionalized dichloronaphthalene (**8**, **10**, and **11**).<sup>9</sup> The sp<sup>2</sup> C–I bonds can be functionalized chemoselectively over the sp<sup>2</sup> C–Cl bonds via Sonogashira cross-coupling with triisopropylsilylacetylene to afford bis-(ethynylated)dichloronaphthalene **9**. The Buchwald–Hartwig amination of dichloronaphthalenes **9–11** with 1,2-diaminobenzene did not afford the dihydroacene product; instead, the fully aromatic diazatetracenes **1–3** were isolated directly. Presumably the reaction proceeds via a dihydroaromatic intermediate that undergoes rapid dehydrogenation to the aromatic system via a Pd-catalyzed dehydrogenation.

Diazatetracenes **1–3** are soluble in common organic solvents such as CH<sub>2</sub>Cl<sub>2</sub>, CHCl<sub>3</sub>, and THF and can be handled under normal laboratory conditions (exposure to air, moisture, and

Received: November 28, 2016

Published: January 19, 2017

Scheme 1. Synthesis of Diazatetracenes 1–3<sup>a</sup>

**Figure 1.** (A) UV-vis absorption of diazatetracenes 1 and 2 in  $\text{CH}_2\text{Cl}_2$  without (solid lines) and with TFA (dashed lines) present. Note: The data for 3 are qualitatively similar to that those of 2 and omitted for clarity (see the Supporting Information). (C) Photograph of diazatetracenes 1 (orange solid) and 2 (red solid) in the solid state. (D) UV-vis absorption and (E) emission spectra ( $\lambda_{\text{exc}} = 414 \text{ nm}$ ) of 2 in  $\text{CH}_2\text{Cl}_2$  in the presence of varying amounts of TFA.

light), including column chromatography. By varying the substituents on the diazatetracene core, we are able to tune their electronic properties, as illustrated by comparing the UV-vis absorption spectra of tetracenes 1 and 2 (Figure 1A–C). The extended conjugation of the additional aryl group and ethynyl groups in 1 provides a red-shift compared to bis-alkylated tetracene 2. Interestingly, there is little difference in the absorption spectra of monomeric derivative 2 and related dimer 3, suggesting little or no  $\pi$ -conjugation across the biaryl

linkage connecting the two diazatetracene chromophores (Table 1). The density functional theory (DFT) optimized geometry using B3LYP/6-31G(d) supports this hypothesis with a dihedral angle for the biaryl linkage of  $81.5^\circ$  (see the Supporting Information for details). The nitrogen atoms embedded in the aromatic chromophore may be reversibly protonated, which changes their absorption and emission spectra dramatically. The addition of excess trifluoroacetic acid (TFA) to a  $\text{CH}_2\text{Cl}_2$  solution of the diazatetracenes causes a red-

Table 1. Summary of Absorption/Emission and Electrochemical Data for Diazatetracenes 1–3<sup>a</sup>

	CH <sub>2</sub> Cl <sub>2</sub>				0.3 M TFA in CH <sub>2</sub> Cl <sub>2</sub>				
	$\lambda_{\text{abs}}$ (nm)	$E_{\text{g}}^{\text{opt}}$ (eV)	$\lambda_{\text{em,max}}$ (nm)	$E_{1/2}^{\text{red1}}$ (V)	$E_{\text{g}}^{\text{electro}}$ (eV)	$\lambda_{\text{abs}}$ (nm)	$E_{\text{g}}^{\text{opt}}$ (eV)	$E_{1/2}^{\text{red1}}$ (V)	$E_{1/2}^{\text{red2}}$ (V)
1	268, 312, 320, 421, 437, 482, 514	2.19	562	-1.16	2.13	281, 324, 494	1.55	-0.05	+0.45
2	255, 293, 392, 414, 483, 511	2.21	573	-1.34	2.04	307, 450, 630	1.55	-0.23	+0.06
3	256, 300, 392, 413, 483, 511	2.21	560	-1.32	1.95	313, 448, 608	1.60	-0.13	+0.47

<sup>a</sup>Solvent is either CH<sub>2</sub>Cl<sub>2</sub> or 0.3 M TFA in CH<sub>2</sub>Cl<sub>2</sub>.  $E_{\text{g}}^{\text{opt}}$  is the optical HOMO–LUMO gap determined from the absorption edge.  $E_{\text{g}}^{\text{electro}}$  is the electrochemical HOMO–LUMO gap determined from the onset of reduction and oxidation. All solutions for electrochemistry experiments contained 0.1 M tetrabutylammonium perchlorate (TBAP) as supporting electrolyte and electrochemical potentials are reported vs Ag/AgClO<sub>4</sub>. Note:  $E_{1/2}^{\text{red1}}$  = half-potential associated with the first reduction process,  $E_{1/2}^{\text{red2}}$  = half-potential associated with the second reduction process,  $E_{\text{onset}}^{\text{ox1}}$  = onset associated with the first oxidation process,  $E_{\text{onset}}^{\text{red1}}$  = onset associated with the first reduction process,  $E_{\text{g}}$  = HOMO–LUMO gap,  $\lambda_{\text{abs}}$  = absorption maxima,  $\lambda_{\text{abs,max}}$  = longest wavelength absorption maxima,  $\lambda_{\text{em,max}}$  = shortest wavelength emission maxima,  $\lambda_{\text{exc}}$  = excitation wavelength.

shift in the absorption features, corresponding to a decrease in the optical HOMO–LUMO gap from ca. 2.2 to 1.6 eV and complete loss in the emission behavior for acenes 1–3. The electronic response is due to lowering of the LUMO energy upon protonation of the chromophore, as evidenced from the electrochemistry experiments described below. Titration experiments using UV–vis absorption and emission spectroscopy were performed to investigate the progression in the optical properties as a function of TFA content in CH<sub>2</sub>Cl<sub>2</sub> solutions of diazatetracene 2 (Figure 1D,E). More than 1 equiv of TFA is required to effect the observed spectroscopic changes. The addition of TFA attenuates the 414 nm UV–vis absorption peak, and a new peak grows in at 450 nm. The photoemission spectra of 2 are also affected by TFA: the emission signal at 573 nm gradually decreases in intensity and is eventually quenched after the addition of 1000–2000 equiv of TFA. This amount of TFA is similar to that needed to effect complete conversion of the UV–vis absorption features. This information, in combination with a literature comparison of pK<sub>a</sub> values of TFA and benzophenazine,<sup>12</sup> suggests that a monoprotonated TFA salt of diazatetracene 2 is formed under these conditions.<sup>13</sup>

Cyclic voltammetry of tetracenes 1–3 (CH<sub>2</sub>Cl<sub>2</sub> with 0.1 M Bu<sub>4</sub>NClO<sub>4</sub> supporting electrolyte) reveals one reduction and one oxidation process (Figure 2). The oxidation process is irreversible (Figure S19, top), while the reduction is quasi-

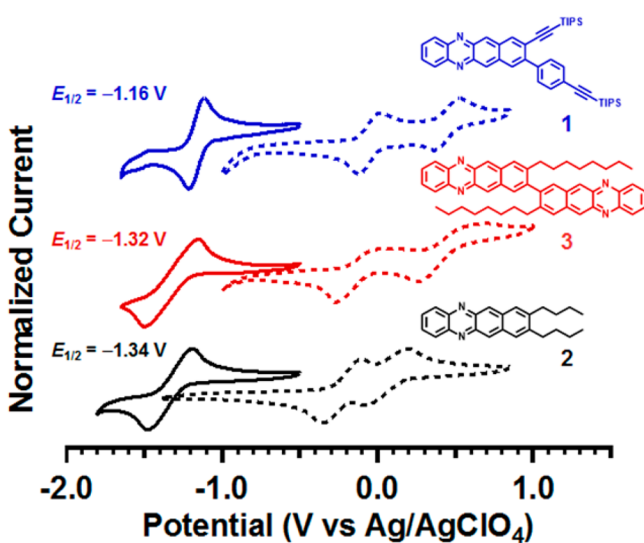


Figure 2. Cyclic voltammetry of diazatetracenes 1–3 (CH<sub>2</sub>Cl<sub>2</sub>/0.1 M Bu<sub>4</sub>NClO<sub>4</sub>/scan rate = 50 mV.s<sup>-1</sup>) without TFA (solid lines) and with 0.3 M TFA (dashed lines).

reversible for 2 and 3 and reversible for 1. The reduction is slightly more facile for derivative 1 ( $E_{1/2}^{\text{red1}} = -1.16$  V), which has extended conjugation compared to the alkylated tetracene monomer 2 ( $E_{1/2}^{\text{red1}} = -1.34$  V). The reduction potential of dimer 3 is located at ( $E_{1/2}^{\text{red1}} = -1.32$  V), which is essentially identical to monomer 1, further consistent with the lack of conjugation between the two diazatetracene moieties. Upon addition of TFA to the diazatetracene solutions, both reduction processes are observed. The first is shifted by more than 1 V to more electropositive potentials, and the second reduction process shifts into the electrochemical window of the electrolyte system. This reduction of the LUMO energy is consistent with protonation of the diazatetracene chromophore. We observed two coupled electron transfers from compounds 1 and 2, as evident from the two distinct redox waves in the CV after the addition of TFA. If the two tetracenes of dimer 3 are electronically coupled, four distinct waves would be observed. Only two waves are observed, suggesting that the two diazatetracene moieties are electronically isolated.

DFT calculations of the diazatetracene chromophore and its TFA-protonated analog reveal the origin for their electronic differences (Figure 3). The HOMO and LUMO of diazatetracene were calculated using the B3LYP functional along with the 6-31G(d) basis set. Protonation leads to a lowering of both the HOMO and LUMO energies as well as a diminished HOMO–LUMO energy gap. These results are consistent with the observed red shift in the absorption spectra and electropositive shift in the reduction potential for compounds 1–3 in the presence of TFA. Protonation of the diazatetracene chromophore leads to a reduction in the orbital coefficient on the ring containing the nitrogen atoms in the HOMO with concomitant increase in the LUMO orbital coefficients at that location. Protonation of the diazatetracene chromophore along with association of a CF<sub>3</sub>COO<sup>-</sup> counterion results in a significant increase the molecular dipole (4.16 D) relative to 0.32 D for neutral diazatetracene. These results are consistent with the electrostatic potential maps shown in Figure 3, in which protonation provides a polarized chromophore with the pyrazine ring decreasing in electron density.

## CONCLUSION

In summary, a new route to diazatetracenes is demonstrated that features the convergent assembly of chlorinated naphthalenes derived from the benzannulation of acetylenes including haloalkynes, butadiynes, or simple dialkylacetylenes. This approach realizes several new structures and substitution patterns, including a dimer and dialkyne derivative amenable for further functionalization or polymerization. The introduction of nitrogen atoms into the tetracene core enables for both

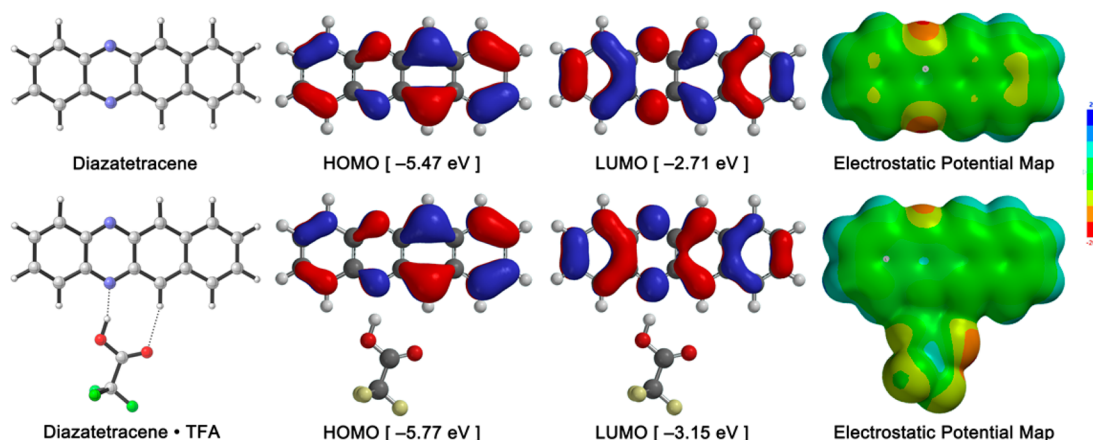


**Figure 3.** Calculated HOMO, LUMO, and electrostatic potential map of diazatetracene (top row) and its TFA monoprotonated salt (bottom row) using B3LYP/6-31G(d). Isovalue = 0.032 for HOMO/LUMO surfaces and 0.002 for the electrostatic potential surface, electrostatic potential scale shown to the right ranges from +200 (blue) to  $-200$  kJ/mol (red).

internal and external tuning of the electronic properties. Their electronic response to Brønsted acids in solution, such as TFA, can likely be extended to Lewis acids to detect metal ions. The ability to modulate the electronic properties of diazatetracenes via protonation or coordination to Lewis acids may also provide a means to control their lowest excited singlet ( $S_1$ ) and triplet state ( $T_1$ ) energies to facilitate singlet fission.<sup>14,15</sup> In fact, dimeric structures such as diazatetracene **3** are exciting candidates for intramolecular singlet fission,<sup>16</sup> especially since the rate of singlet fission can increase when nitrogen atoms are incorporated into aromatic cores.<sup>7</sup> We anticipate that this synthetic method will provide access to new heteroatom-containing PAHs, including their respective oligomers, with useful properties for organic electronic devices ranging from photovoltaics to sensing and potential organic photosensitizers with complementary properties to acridinium-based motifs.<sup>17</sup>

## EXPERIMENTAL SECTION

Reagents were purchased in reagent grade from commercial suppliers and used without further purification. Compounds **4**, **5**, and **8** were synthesized using a literature procedure,<sup>9</sup> and compound **6** was commercially available and used as received. All reactions were performed in standard, dry glassware fitted with a rubber septum under an inert atmosphere of nitrogen, unless otherwise described. Stainless steel syringes or cannulae were used to transfer air- and moisture-sensitive liquids. Anhydrous solvents ( $\text{CH}_2\text{Cl}_2$ , toluene, THF, DMF) were obtained from a solvent purification system. Evaporation and concentration in vacuo were performed using variable vacuum-controlled pumps (ca. 400–40 mmHg). Column chromatography was done using a standard flash chromatography technique using SiliaFlash P60 silica gel (40–63  $\mu\text{m}$ , 230–400 mesh) from Silicycle and pressurized (ca. 30–50 psi) using compressed air. Thin-layer chromatography (TLC) was used for reaction monitoring and product detection using precoated glass plates covered with 0.20 mm silica gel with fluorescent indicator UV 254 nm and visualization by UV light or  $\text{KMnO}_4$  stain. Proton nuclear magnetic resonance ( $^1\text{H}$  NMR) spectra and carbon nuclear magnetic resonance ( $^{13}\text{C}$  NMR) spectra were recorded at 25  $^\circ\text{C}$  (unless stated otherwise). Chemical shifts for protons are reported in parts per million downfield from tetramethylsilane and are referenced to residual protium in the NMR solvent according to values reported in the literature.<sup>18</sup> Chemical shifts for carbon are reported in parts per million downfield from tetramethylsilane and are referenced to the carbon resonances of the solvent. The solvent peak was referenced to 7.26 ppm for  $^1\text{H}$  and 77.0 ppm for  $^{13}\text{C}$  for  $\text{CDCl}_3$ . Data are represented as follows: chemical shift, integration, multiplicity (br = broad, s = singlet, d = doublet, t =

triplet, q = quartet, m = multiplet), coupling constants in hertz (Hz). In the case of compounds containing one or more fluorine atom(s), it should be noted that  $^{13}\text{C}$  NMR experiments were obtained in which only the  $^1\text{H}$  nuclei was decoupled, (i.e.,  $^{13}\text{C}\{^1\text{H}\}$ ). Infrared spectra were recorded using an FT-IR spectrometer equipped with a diamond ATR. Data are represented as follows: frequency of absorption ( $\text{cm}^{-1}$ ), intensity of absorption (s = strong, m = medium, w = weak, vw = very weak, br = broad). High-resolution mass spectrometry was measured using a direct analysis in real time (DART) mass spectrometer equipped with an orbitrap mass analyzer, sample introduction was carried out by coating the outer walls of a capillary melting point tube with the sample solution (typically in  $\text{CDCl}_3$  or  $\text{CH}_2\text{Cl}_2$ ) and exposing such tubes to the sample inlet port. All absorption and emission spectra were recorded at rt in the presence of air. Electrochemistry experiments were performed with the analyte dissolved in dichloromethane with recrystallized tetrabutylammonium perchlorate (TBAP) as the supporting electrolyte (0.1 M). A three-electrode cell was used with a glassy carbon working electrode and a platinum wire counter electrode. Silver/silver ion (Ag) in 0.05 M  $\text{AgClO}_4$ , 0.1 M TBAP solution in MeCN) was used as a reference electrode. The potential values ( $E$ ) were calculated using the equation (except where otherwise noted)  $E^{1/2} = (E_{\text{pc}} + E_{\text{pa}})/2$ , where  $E_{\text{pc}}$  and  $E_{\text{pa}}$  correspond to the cathodic and anodic peak potentials, respectively. Solution cyclic voltammetry was performed in ca. 1–5 mM solutions of diazatetracene derivatives in  $\text{CH}_2\text{Cl}_2$  containing 0.1 M TBAP as supporting electrolyte. All solutions were deoxygenated with argon before each experiment, and a blanket of argon was used over the solution during the experiment. Density function theory calculations were performed using either Gaussian 09<sup>19</sup> or Spartan<sup>14</sup>.<sup>20</sup>

**Compound 1.** A suspension of **9** (0.160 g, 0.252 mmol), 1,2-diaminobenzene (0.028 g, 0.254 mmol), SPhos (0.010 g, 0.025 mmol, SPhos = 2-dicyclohexylphosphino-2',6'-dimethoxybiphenyl),  $\text{Pd}(\text{OAc})_2$  (0.006 g, 0.025 mmol), and  $\text{Cs}_2\text{CO}_3$  (0.271 g, 0.833 mmol) in toluene (2.5 mL) was deoxygenated via sparging with  $\text{N}_2$  for 5 min followed by heating in an oil bath to 110  $^\circ\text{C}$  for 12 h. The mixture was cooled to rt and diluted with  $\text{CH}_2\text{Cl}_2$ , the organic phase was washed with 5% aq  $\text{NH}_4\text{Cl}$  (2 $\times$ ), dried over  $\text{Na}_2\text{SO}_4$ , and filtered, and the solvent was removed in vacuo. Column chromatography (silica gel, 2:10:88  $\text{Et}_3\text{N}/\text{CH}_2\text{Cl}_2/\text{hexanes}$ ) afforded **1** (0.117 g, 70%) as a red solid.  $R_f = 0.5$  (2:10:88  $\text{Et}_3\text{N}/\text{CH}_2\text{Cl}_2/\text{hexanes}$ ). IR ( $\text{CDCl}_3$ , cast film): 2942 (s), 2891 (m), 2865 (s), 2153 (m), 1484 (w), 1464 (m), 1377 (w), 1365 (w), 1222 (w), 1130 (w), 1112 (w), 1073 (w), 1017 (w), 996 (m), 906 (m), 883 (m), 834 (m), 789 (m), 754 (m), 705 (w), 677 (m), 661 (m)  $\text{cm}^{-1}$ .  $^1\text{H}$  NMR (300 MHz,  $\text{CDCl}_3$ ):  $\delta$  8.88 (s, 2H), 8.42 (s, 1H), 8.26–8.19 (m, 2H), 8.05 (s, 1H), 7.83 (dd,  $J = 6.9, 3.3$  Hz, 1H), 7.66 (d,  $J = 8.0$  Hz, 1H), 7.56 (d,  $J = 8.2$  Hz, 1H), 1.19–1.14 (m, 21H), 1.08–1.03 (m, 21H).  $^{13}\text{C}$  NMR (125 MHz,  $\text{CDCl}_3$ ):  $\delta$  144.7, 140.8, 140.6, 140.6, 139.7, 134.3, 133.6, 133.1, 131.6, 131.0,

131.0, 129.9, 129.3, 128.1, 127.8, 127.3, 123.0, 122.1, 107.1, 105.8, 98.0, 91.3, 77.3, 77.0, 76.7, 18.7, 18.6, 11.3, 11.3. DART HRMS:  $m/z$  calcd for  $C_{44}H_{35}N_2Si_2$  ( $[M + H]^+$ ) 667.3898, found 667.3866.

**Compound 2.** A suspension of **10** (0.336 g, 1.09 mmol), 1,2-diaminobenzene (0.118 g, 1.09 mmol), SPhos (0.045 g, 0.11 mmol), Pd(OAc)<sub>2</sub> (0.024 g, 0.11 mmol), and Cs<sub>2</sub>CO<sub>3</sub> (1.17 g, 3.59 mmol) in toluene (4.3 mL) was deoxygenated via sparging with N<sub>2</sub> for 5 min followed by heating in an oil bath to 110 °C for 12 h. The mixture was cooled to rt and diluted with CH<sub>2</sub>Cl<sub>2</sub>, the organic phase was washed with 5% aq NH<sub>4</sub>Cl (2×), dried over Na<sub>2</sub>SO<sub>4</sub>, filtered, and the solvent was removed in vacuo. Column chromatography (silica gel, 2:20:78 Et<sub>3</sub>N/CH<sub>2</sub>Cl<sub>2</sub>/hexanes) followed by recrystallization (sample was dissolved in minimal amount of CH<sub>2</sub>Cl<sub>2</sub> followed by addition of hexanes at rt, and then the mixture was cooled to -78 °C, filtered, and washed with hexanes) afforded **2** (0.101 g, 27%) as a dark red solid.  $R_f$  = 0.2 (2:20:78 Et<sub>3</sub>N/CH<sub>2</sub>Cl<sub>2</sub>/hexanes). IR (CDCl<sub>3</sub> cast film): 3408 (w), 3059 (w), 2953 (s), 2928 (s), 2869 (m), 1637 (w), 1586 (w), 1491 (w), 1456 (s), 1382 (m), 1297 (w), 1261 (w), 1113 (m), 937 (w), 890 (m), 814 (w), 750 (s) cm<sup>-1</sup>. <sup>1</sup>H NMR (500 MHz, CDCl<sub>3</sub>): δ 8.75 (s, 2H), 8.24–8.16 (m, 2H), 7.85 (s, 2H), 7.80–7.73 (s, 2H), 2.83 (t,  $J$  = 7.3 Hz, 4H), 1.80–1.69 (m, 4H), 1.52 (sextet,  $J$  = 7.0 Hz, 4H), 1.02 (t,  $J$  = 7.0 Hz, 6H). <sup>13</sup>C NMR (125 MHz, CDCl<sub>3</sub>): δ 144.2, 141.9, 140.1, 134.2, 130.2, 129.8, 126.5, 125.9, 32.8, 22.9, 14.0. DART HRMS:  $m/z$  calcd for C<sub>24</sub>H<sub>27</sub>N<sub>2</sub> ( $[M + H]^+$ ) 343.2169, found 343.2160.

**Compound 3.** A suspension of **11** (0.423 g, 0.686 mmol), 1,2-diaminobenzene (0.163 g, 1.51 mmol), SPhos (0.048 g, 0.117 mmol), Pd(OAc)<sub>2</sub> (0.026 g, 0.117 mmol), and Cs<sub>2</sub>CO<sub>3</sub> (1.48 g, 4.53 mmol) in toluene (4.6 mL) was deoxygenated via sparging with N<sub>2</sub> for 5 min followed by heating in an oil bath to 110 °C for 12 h. The mixture was cooled to rt and diluted with CH<sub>2</sub>Cl<sub>2</sub>, the organic phase was washed with 5% aq NH<sub>4</sub>Cl (2×), dried over Na<sub>2</sub>SO<sub>4</sub>, filtered, and the solvent was removed in vacuo. The crude was diluted in CH<sub>2</sub>Cl<sub>2</sub>, and the solution was partitioned into two equal portions:

The first portion was concentrated in vacuo and purified by column chromatography (silica gel, 3:20:77 Et<sub>3</sub>N/CH<sub>2</sub>Cl<sub>2</sub>/hexanes) to afford **3** (0.074 g, 32%) as a bright orange solid. The second portion was concentrated in vacuo, the residue was suspended in 10:1 v/v AcOH/H<sub>2</sub>O (20 mL), K<sub>2</sub>Cr<sub>2</sub>O<sub>7</sub> (0.404 g, 1.37 mmol) was added, and the mixture was stirred for 4 h at rt. The mixture was diluted with CH<sub>2</sub>Cl<sub>2</sub>, the organic phase was washed with 5% aq Na<sub>2</sub>CO<sub>3</sub> (2×), dried over Na<sub>2</sub>SO<sub>4</sub>, and filtered, and the solvent was removed in vacuo. Column chromatography (silica gel, 2:20:78 Et<sub>3</sub>N/CH<sub>2</sub>Cl<sub>2</sub>/hexanes) afforded **3** (0.039 g, 17%) as a bright orange solid. Material obtained via this oxidation step had spectral characterization consistent with material obtained without this oxidation step (i.e., material from the first portion, as described above).

**Characterization of 3.**  $R_f$  = 0.5 (20% CH<sub>2</sub>Cl<sub>2</sub> in hexanes). IR (DCM cast film): 3418 (vw), 3050 (w), 2953 (w), 2922 (m), 2851 (w), 1526 (w), 1491 (w), 1455 (w), 1408 (w), 1381 (m), 1108 (m), 972 (w), 918 (w), 897 (s), 833 (w), 773 (w), 750 (s), 727 (w), 668 (w) cm<sup>-1</sup>. <sup>1</sup>H NMR (500 MHz, CDCl<sub>3</sub>): δ 8.93 (s, 2H), 8.92 (s, 2H), 8.28–8.21 (m, 4H), 8.08 (s, 2H), 8.06 (s, 2H), 7.84–7.78 (m, 4H), 2.73–2.50 (m, 4H), 1.66–1.58 (m, 4H), 1.25–0.98 (m, 20H), 0.69 (t,  $J$  = 7.0 Hz, 6H). <sup>13</sup>C NMR (500 MHz): δ 144.6, 144.4, 141.25, 141.15, 140.5, 140.3, 134.6, 133.5, 130.7, 130.6, 129.92, 129.89, 128.8, 127.3, 126.6, 126.5, 33.9, 31.7, 30.3, 29.4, 29.2, 29.0, 22.5, 14.0. DART HRMS:  $m/z$  calcd for C<sub>48</sub>H<sub>51</sub>N<sub>4</sub> ( $[M + H]^+$ ) 683.4108, found 683.4114.

**Compound 7.**<sup>21</sup> To a round-bottom flask containing CuCl (0.730 g, 0.738 mmol) were added *n*-BuNH<sub>2</sub> (7.29 mL, 5.40 g, 73.8 mmol), H<sub>2</sub>O (11.1 mL, 11.1 g, 615 mmol), and CH<sub>2</sub>Cl<sub>2</sub> (40 mL) in that order, and the solution was cooled to 0 °C accompanied by vigorous stirring. The mixture was deoxygenated via sparging with nitrogen for 3 min followed by addition of small amounts of NH<sub>2</sub>OH·HCl until complete decolorization of the initial blue mixture was achieved. At that time, a deoxygenated solution of 1-bromodec-1-yne (1.47 g, 6.76 mmol) in CH<sub>2</sub>Cl<sub>2</sub> (20 mL) was added dropwise. The reaction mixture was stirred for 3 h at 0 °C, followed by removal of the cooling bath and aging of the mixture at rt for another 6 h before it was poured into 5%

aq NH<sub>4</sub>Cl. H<sub>2</sub>O was added, and the mixture was extracted with CH<sub>2</sub>Cl<sub>2</sub> (100 mL). The organic phase was washed with 5% aq NH<sub>4</sub>Cl and satd aq NaHCO<sub>3</sub> and dried (Na<sub>2</sub>SO<sub>4</sub>), and the solvent was removed in vacuo. Column chromatography (silica gel, hexanes) afforded **7** (1.12 g, 66%) as a pale yellow liquid. Spectral data were consistent with previously reported data.<sup>21</sup>

**1-Bromodec-1-yne.**<sup>22</sup> To a solution of 1-decyne (2.00 g, 2.61 mL, 14.5 mmol) in acetone (50 mL) at rt was added *N*-bromosuccinimide (2.96 g, 16.6 mmol) followed by AgNO<sub>3</sub> (0.246 g, 1.45 mmol). The mixture was stirred at rt for 2 h in the dark (via wrapping the reaction flask in aluminum foil). The mixture was then filtered through a pad of silica gel using hexanes. The filtrate was collected, and the solvent was removed in vacuo. Column chromatography (silica gel, hexanes) afforded 1-bromodec-1-yne (1.47 g, 47%) as a clear colorless liquid.  $R_f$  = 0.7 (hexanes). IR (CDCl<sub>3</sub> cast film): 2955 (m), 2926 (s), 2855 (s), 2218 (vw), 1466 (m), 1430 (w), 1328 (w), 1053 (w), 909 (m), 736 (m) cm<sup>-1</sup>. <sup>1</sup>H NMR (300 MHz, CDCl<sub>3</sub>): δ 2.19 (t,  $J$  = 7.0 Hz, 2H), 1.51 (quintet,  $J$  = 7.0 Hz, 2H), 1.42–1.22 (m, 10H), 0.88 (t,  $J$  = 6.7 Hz, 3H). <sup>13</sup>C NMR (100 MHz, CDCl<sub>3</sub>): δ 80.2, 37.4, 31.9, 29.2, 29.1, 28.8, 28.4, 22.7, 19.7, 14.0. DART HRMS:  $m/z$  calcd for C<sub>10</sub>H<sub>17</sub><sup>79</sup>Br ( $[M - Br]^+$ ) 137.1325, found 137.1328.

**Compound 9.** To a flask containing Pd(PPh<sub>3</sub>)<sub>4</sub> (0.053 g, 0.046 mmol) and CuI (0.012 g, 0.061 mmol) under an atmosphere of nitrogen was added via cannula a solution of **8**<sup>9</sup> (0.400 g, 0.762 mmol) in THF (10 mL) and diisopropylamine (1.6 mL, 1.2 g, 12 mmol) which had been deoxygenated via sparging with N<sub>2</sub> for 10 min. To the combined mixture was added triisopropylsilylacetylene (0.46 mL, 0.38 g, 2.1 mmol) while the mixture was sparged with N<sub>2</sub> for another 2 min. The mixture was stirred for 12 h at rt before being diluted with CH<sub>2</sub>Cl<sub>2</sub>. The organic phase was washed with H<sub>2</sub>O and satd aq NH<sub>4</sub>Cl, dried over anhyd Na<sub>2</sub>SO<sub>4</sub>, and filtered through a short pad of silica gel (using CH<sub>2</sub>Cl<sub>2</sub> as eluent), and the solvent was removed in vacuo. Column chromatography (silica gel, hexanes) gave **9** (0.699 g, 92%) as a white solid.  $R_f$  = 0.5 (hexanes). IR (CDCl<sub>3</sub> cast film): 2941 (m), 2890 (w), 2864 (m), 2154 (w), 1510 (w), 1469 (m), 1383 (w), 1345 (w), 1226 (w), 1182 (w), 1120 (m), 1019 (w), 996 (w), 970 (m), 907 (m), 882 (m), 834 (m), 779 (m), 738 (w), 716 (m), 665 (s) cm<sup>-1</sup>. <sup>1</sup>H NMR (400 MHz, CDCl<sub>3</sub>): δ 8.00 (s, 1H), 7.89 (s, 2H), 7.65 (s, 1H), 7.59–7.52 (m, 4H), 1.18 (s, 21H), 1.06 (s, 21H). <sup>13</sup>C NMR (100 MHz, CDCl<sub>3</sub>): δ 141.6, 139.7, 132.4, 131.64, 131.57, 131.3, 130.94, 130.89, 129.3, 128.7, 128.1, 126.8, 123.0, 121.7, 107.1, 105.4, 96.5, 91.2, 18.7, 18.5, 11.4, 11.3. DART HRMS:  $m/z$  calcd for C<sub>38</sub>H<sub>51</sub>Si<sub>2</sub><sup>35</sup>Cl<sub>2</sub> ( $[M + H]^+$ ) 633.2901, found 633.2890.

**Compound 10.** A solution of 5-decyne (0.168 g, 1.22 mmol) and **4** (0.449 g, 1.63 mmol) in 1,2-dichloroethane (23.8 mL) which had been deoxygenated via sparging with N<sub>2</sub> for 5 min was transferred via cannula into a round-bottom flask equipped with a water-cooled condenser containing Cu(OTf)<sub>2</sub> (0.044 g, 0.122 mmol) under nitrogen atmosphere, and additional 1,2-dichloroethane (0.5 mL) was used to complete the solution transfer. TFA (0.47 mL, 0.69 g, 6.1 mmol) was immediately added. The mixture was heated in an oil bath to 100 °C for 2 h. The mixture cooled to rt, NaHCO<sub>3</sub> (ca. 2 g) was added, and the mixture was filtered through a short pad of silica gel using 1:1 hexanes/CH<sub>2</sub>Cl<sub>2</sub>. The solvent from the filtrate was removed in vacuo. Column chromatography (silica gel, hexanes) afforded **10** (0.358 g, 95%) as a white solid.  $R_f$  = 0.8 (hexanes). IR (CDCl<sub>3</sub> cast film): 2953 (s), 2930 (s), 2870 (m), 1582 (w), 1485 (m), 1464 (m), 1439 (m), 1379 (m), 1356 (m), 1221 (w), 1188 (w), 1175 (w), 1118 (s), 971 (s), 938 (m), 905 (s), 890 (s), 759 (w), 736 (w), 658 (m) cm<sup>-1</sup>. <sup>1</sup>H NMR (500 MHz, CDCl<sub>3</sub>): δ 7.81 (s, 2H), 7.47 (s, 2H), 2.79 (t,  $J$  = 7.9 Hz, 4H), 1.71 (quintet,  $J$  = 7.6 Hz, 4H), 1.54 (sextet,  $J$  = 7.3 Hz, 4H), 1.09 (t,  $J$  = 7.3 Hz, 6H). <sup>13</sup>C NMR (125 MHz, CDCl<sub>3</sub>): δ 140.9, 131.0, 128.8, 127.8, 125.6, 32.9, 32.4, 22.8, 14.0. DART HRMS:  $m/z$  calcd for C<sub>18</sub>H<sub>22</sub><sup>35</sup>Cl<sub>2</sub> (M<sup>+</sup>) 308.1093, found 308.1086.

**Compound 11.** A solution of **7** (0.287 g, 1.05 mmol) and **4** (0.777 g, 2.82 mmol) in 1,2-dichloroethane (16.9 mL) which had been deoxygenated via sparging with N<sub>2</sub> for 5 min was transferred via cannula into a round-bottom flask equipped with a water-cooled condenser containing Cu(OTf)<sub>2</sub> (0.038 g, 0.105 mmol) under nitrogen atmosphere, and additional 1,2-dichloroethane (0.5 mL)

was used to complete the solution transfer. TFA (0.40 mL, 0.60 g, 5.2 mmol) was immediately added. The mixture was heated in an oil bath to 100 °C for 2 h. The mixture was cooled to rt, NaHCO<sub>3</sub> (ca. 2 g) was added, and the mixture was filtered through a short pad of silica gel using 1:1 hexanes/CH<sub>2</sub>Cl<sub>2</sub>. The solvent from the filtrate was removed in vacuo. Column chromatography (silica gel, hexanes) afforded **11** (0.451 g, 70%) as a white solid. *R<sub>f</sub>* = 0.7 (hexanes). IR (DCM cast film): 2953 (m), 2925 (s), 2854 (m), 1579 (w), 1473 (m), 1433 (w), 1391 (w), 1378 (w), 1346 (w), 1184 (w), 1119 (s), 972 (m), 961 (w), 906 (s), 738 (m), 662 (m) cm<sup>-1</sup>. <sup>1</sup>H NMR (500 MHz, CDCl<sub>3</sub>): δ 7.94 (s, 2H), 7.88 (s, 2H), (s, 2H), 7.69 (s, 2H), 7.57 (s, 2H), 2.61–2.39 (m, 4H), 1.57–1.47 (m, 4H), 1.26–1.06 (m, 20H), 0.86 (t, *J* = 7.2 Hz, 3H). <sup>13</sup>C NMR (500 MHz, CDCl<sub>3</sub>): δ 140.7, 140.4, 132.0, 130.4, 130.1, 129.6, 128.3, 128.1, 127.4, 125.8, 33.3, 31.8, 30.4, 29.3, 29.2, 29.1, 22.6, 14.1. DART HRMS: *m/z* calcd for C<sub>36</sub>H<sub>42</sub><sup>35</sup>Cl<sub>4</sub> (M<sup>+</sup>) 614.2035, found 614.2061.

## ■ ASSOCIATED CONTENT

### 📄 Supporting Information

The Supporting Information is available free of charge on the ACS Publications website at DOI: 10.1021/acs.joc.6b02840.

<sup>1</sup>H and <sup>13</sup>C NMR spectra, Cartesian coordinates of the DFT structure, and additional data (PDF)

## ■ AUTHOR INFORMATION

### Corresponding Author

\*E-mail: wdichtel@northwestern.edu.

### ORCID

Catherine R. Mulzer: 0000-0002-4013-4025

William R. Dichtel: 0000-0002-3635-6119

### Notes

The authors declare no competing financial interest.

## ■ ACKNOWLEDGMENTS

This research was supported by the NSF (CHE-1124754) and the Beckman Young Investigator Program. C.R.M. was supported by an NSF GRFP (DGE-1144153). This work made use of the Cornell Center for Materials Research Shared Facilities which are supported through the NSF MRSEC program (DMR-1120296).

## ■ REFERENCES

- (1) (a) Anthony, J. E. *Angew. Chem., Int. Ed.* **2008**, *47*, 452–483. (b) Anthony, J. E. *Chem. Rev.* **2006**, *106*, 5028–5048. (c) Bendikov, M.; Wudl, F.; Perepichka, D. F. *Chem. Rev.* **2004**, *104*, 4891–4945. (d) Lehnher, D.; Tykwinski, R. R. *Aust. J. Chem.* **2011**, *64*, 919–929. (e) Jiang, W.; Li, Y.; Wang, Z. *Chem. Soc. Rev.* **2013**, *42*, 6113–6127. (f) *Polycyclic Arenes and Heteroarenes: Synthesis, Properties, and Applications*; Miao, Q., Ed.; John Wiley & Sons: New York, 2015.
- (2) (a) Laquindanum, J. G.; Katz, H. E.; Lovinger, A. J. *J. Am. Chem. Soc.* **1998**, *120*, 664–672. (b) Lehnher, D.; Waterloo, A. R.; Goetz, K. P.; Payne, M. M.; Hampel, F.; Anthony, J. E.; Jurchescu, O. D.; Tykwinski, R. R. *Org. Lett.* **2012**, *14*, 3660–3663. (c) Takimiya, K.; Nakano, M.; Kang, M. J.; Miyazaki, E.; Osaka, I. *Eur. J. Org. Chem.* **2013**, *2013*, 217–227.
- (3) (a) Nakano, M.; Niimi, K.; Miyazaki, E.; Osaka, I.; Takimiya, K. *J. Org. Chem.* **2012**, *77*, 8099–8111. (b) Watanabe, M.; Doi, Y.; Hagiwara, H.; Staykov, A. T.; Ida, S.; Matsumoto, T.; Shinmyozu, T.; Ishihara, T. *J. Org. Chem.* **2015**, *80*, 9159–9166. (c) Wang, S.; Lv, B.; Cui, Q.; Ma, X.; Ba, X.; Xiao, J. *Chem. - Eur. J.* **2015**, *21*, 14791–14796. (d) VanVeller, B.; Robinson, D.; Swager, T. M. *Angew. Chem., Int. Ed.* **2012**, *51*, 1182–1186. (e) Stassen, D.; Demitri, N.; Bonifazi, D. *Angew. Chem., Int. Ed.* **2016**, *55*, 5947–5951.
- (4) (a) Caruso, A., Jr.; Siegler, M. A.; Tovar, J. D. *Angew. Chem., Int. Ed.* **2010**, *49*, 4213–4217. (b) Neue, B.; Araneda, J. F.; Piers, W. E.;

Parvez, M. *Angew. Chem., Int. Ed.* **2013**, *52*, 9966–9969. (c) Wang, X.-Y.; Wang, J.-Y.; Pei, J. *Chem. - Eur. J.* **2015**, *21*, 3528–3539. (d) Morgan, M. M.; Piers, W. E. *Dalton Trans.* **2016**, *45* (14), 5920–5924. (e) Jäkle, F. *Top. Organomet. Chem.* **2015**, *49*, 297–325.

(5) (a) Bunz, U. H. F. *Chem. - Eur. J.* **2016**, *22*, 4680–4689. (b) Bunz, U. H. F.; Engelhart, J. U.; Lindner, B. D.; Schaffroth, M. *Angew. Chem., Int. Ed.* **2013**, *52*, 3810–3821. (c) Bunz, U. H. F. *Chem. - Eur. J.* **2009**, *15*, 6780–6789. (d) Miao, Q. *Synlett* **2012**, *23*, 326–336. (e) Balandier, J.-Y.; Henry, N.; Arlin, J.-B.; Sanguinet, L.; Lemaury, V.; Niebel, C.; Chattopadhyay, B.; Kennedy, A. R.; Leriche, P.; Blanchard, P.; Cornil, J.; Geerts, Y. H. *Org. Lett.* **2013**, *15*, 302–305. (f) Antonicelli, G.; Gozalvez, C.; Atxabal, A.; Melle-Franco, M.; Hueso, L. E.; Mateo-Alonso, A. *Org. Lett.* **2016**, *18*, 4694–4697. (g) Granger, D. B.; Mei, Y.; Thorley, K. J.; Parkin, S. R.; Jurchescu, O. D.; Anthony, J. E. *Org. Lett.* **2016**, *18*, 6050–6053.

(6) (a) Stepien, M.; Gońka, E.; Żyła, M.; Sprutta, N. *Chem. Rev.* **2016**, DOI: 10.1021/acs.chemrev.6b00076. (b) Jiang, W.; Wang, Z. *Chem. Soc. Rev.* **2013**, *42*, 6113–6127. (c) Wang, C.; Dong, H.; Hu, W.; Liu, Y.; Zhu, D. *Chem. Rev.* **2012**, *112*, 2208–2267. (d) Thomas, S. W.; Joly, G. D.; Swager, T. M. *Chem. Rev.* **2007**, *107*, 1339–1386. (e) Mike, J. F.; Lutkenhaus, J. L. *J. Polym. Sci., Part B: Polym. Phys.* **2013**, *51*, 468–480. (f) Schön, T. B.; McAllister, B. T.; Li, P.-F.; Seferos, D. S. *Chem. Soc. Rev.* **2016**, *45*, 6345–6404. (g) Takimiya, K.; Shinamura, S.; Osaka, I.; Miyazaki, E. *Adv. Mater.* **2011**, *23*, 4347–4370. (h) Zhang, G.; Lan, Z.-A.; Wang, X. *Angew. Chem., Int. Ed.* **2016**, *55*, 15712–15727.

(7) Herz, J.; Buckup, T.; Paulus, F.; Engelhart, J. U.; Bunz, U. H. F.; Motzkus, M. *J. Phys. Chem. Lett.* **2014**, *5*, 2425–2430.

(8) (a) Smith, M. B.; Michl, J. *Chem. Rev.* **2010**, *110*, 6891–6936. (b) Johnson, J. C.; Nozik, A. J.; Michl, J. *Acc. Chem. Res.* **2013**, *46*, 1290–1299. (c) Low, J. Z.; Sanders, S. N.; Campos, L. M. *Chem. Mater.* **2015**, *27*, 5453–5463. (d) Xia, J.; Sanders, S. N.; Cheng, W.; Low, J. Z.; Liu, J.; Campos, L.; Sun, T. *Adv. Mater.* **2016**, 1601652.

(9) Lehnher, D.; Alzola, J. M.; Lobkovsky, E. B.; Dichtel, W. R. *Chem. - Eur. J.* **2015**, *21*, 18122–18127.

(10) For related methodology utilizing Cu or Au catalysis, see: (a) Asao, N.; Nogami, T.; Lee, S.; Yamamoto, Y. *J. Am. Chem. Soc.* **2003**, *125*, 10921–10925. (b) Asao, N.; Takahashi, K.; Lee, S.; Kasahara, T.; Yamamoto, Y. *J. Am. Chem. Soc.* **2002**, *124*, 12650–12651.

(11) For examples of benzannulation chemistry in oligomeric and polymeric settings, see: (a) Gao, J.; Uribe-Romo, F. J.; Saathoff, J. D.; Arslan, H.; Crick, C. R.; Hein, S. J.; Itin, B.; Clancy, P.; Dichtel, W. R.; Loo, Y.-L. *ACS Nano* **2016**, *10*, 4847–4856. (b) Lehnher, D.; Chen, C.; Pedramrazi, Z.; DeBlase, C. R.; Alzola, J. M.; Keresztes, I.; Lobkovsky, E. B.; Crommie, M. F.; Dichtel, W. R. *Chem. Sci.* **2016**, *7*, 6357–6364. (c) Arslan, H.; Saathoff, J. D.; Bunck, D. N.; Clancy, P.; Dichtel, W. R. *Angew. Chem., Int. Ed.* **2012**, *51*, 12051–12054.

(12) (a) Milne, J. B.; Parker, T. J. *J. Solution Chem.* **1981**, *10*, 479–487. (b) Mordziński, A.; Grabowska, A. *J. Lumin.* **1981**, *23*, 393–404. (c) Del Barrio, J. I.; Rebato, J. R.; G.-Tablas, F. M. *J. Phys. Chem.* **1989**, *93*, 6836–6837.

(13) The ground-state p*K<sub>a</sub>* values of mono- and bis-protonated benzophenazine were reported to be 1.52 and –4.15, respectively, as described in reference 12b. The ground state p*K<sub>a</sub>* of mono- and bis-protonated phenazine were reported to be 1.21 and –4.30, respectively, as described in reference 12c. It is reasonable to conclude that TFA (p*K<sub>a</sub>* = 0.23) is not a strong enough acid to generate bis-protonated diazatetracene **2**, thus the monoprotated form of **2** is responsible for the observed changes in the UV–vis absorption/emission spectra and cyclic voltammograms when **2** is exposed to TFA.

(14) Singlet fission requires that the energy of S<sub>1</sub> must be higher than twice the energy of T<sub>1</sub>.

(15) For related examples of modulating electronic properties via external stimuli, see (a) Schneider, J. A.; Perepichka, D. F. *J. Mater. Chem. C* **2016**, *4*, 7269–7276. (b) Hines, D. A.; Darzi, E. R.; Hirst, E. S.; Jasti, R.; Kamat, P. V. *J. Phys. Chem. A* **2015**, *119*, 8083–8089. (c) Welch, G. C.; Bazan, G. C. *J. Am. Chem. Soc.* **2011**, *133*, 4632–

4644. (d) Hansmann, M. M.; López-Andarias, A.; Rettenmeier, E.; Egler-Lucas, C.; Rominger, F.; Hashmi, A. S. K.; Romero-Nieto, C. *Angew. Chem., Int. Ed.* **2016**, *55*, 1196–1199. (e) Cai, K.; Yan, Q.; Zhao, D. *Chem. Sci.* **2012**, *3*, 3175–3182. (f) Matsui, K.; Segawa, Y.; Itami, K. *Org. Lett.* **2012**, *14*, 1888–1891. (g) Huynh, H. V.; He, X.; Baumgartner, T. *Chem. Commun.* **2013**, *49*, 4899–4901.

(16) For selected examples of intramolecular singlet fission, see: (a) Zirzmeier, J.; Lehnher, D.; Coto, P. B.; Chernick, E. T.; Casillas, R.; Basel, B.; Thoss, M.; Tykwinski, R. R.; Guldi, D. M. *Proc. Natl. Acad. Sci. U. S. A.* **2015**, *112*, 5325–5330. (b) Sanders, S. N.; Kumarasamy, E.; Pun, A. B.; Trinh, M. T.; Choi, B.; Xia, J.; Taffet, E. J.; Low, J. Z.; Miller, J. R.; Roy, X.; Zhu, X.-Y.; Steigerwald, M. L.; Sfeir, M. Y.; Campos, L. M. *J. Am. Chem. Soc.* **2015**, *137*, 8965–8972. (c) Sanders, S. N.; Kumarasamy, E.; Pun, A. B.; Steigerwald, M. L.; Sfeir, M. Y.; Campos, L. M. *Angew. Chem., Int. Ed.* **2016**, *55*, 3373–3377. (d) Margulies, E. A.; Miller, C. E.; Wu, Y.; Ma, L.; Schatz, G. C.; Young, R. M.; Wasielewski, M. R. *Nat. Chem.* **2016**, *8*, 1120–1125. (e) Korovina, N. V.; Das, S.; Nett, Z.; Feng, X.; Joy, J.; Haiges, R.; Krylov, A. I.; Bradforth, S. E.; Thompson, M. E. *J. Am. Chem. Soc.* **2016**, *138*, 617–627. (f) Tayebjee, M. J. Y.; Sanders, S. N.; Kumarasamy, E.; Campos, L. M.; Sfeir, M. Y.; McCamey, D. R. *Nat. Phys.* **2016**, DOI: 10.1038/nphys3909. (g) Zirzmeier, J.; Casillas, R.; Reddy, S. R.; Coto, P. B.; Lehnher, D.; Chernick, E. T.; Papadopoulos, I.; Thoss, M.; Tykwinski, R. R.; Guldi, D. M. *Nanoscale* **2016**, *8*, 10113–10123.

(17) (a) Romero, N. A.; Margrey, K. A.; Tay, N. E.; Nicewicz, D. A. *Science* **2015**, *349*, 1326–1330. (b) Romero, N. A.; Nicewicz, D. A. *Chem. Rev.* **2016**, *116*, 10075–10166. (c) Joshi-Pangu, A.; Lévesque, F.; Roth, H. G.; Oliver, S. F.; Campeau, L.-C.; Nicewicz, D.; DiRocco, D. A. *J. Org. Chem.* **2016**, *81*, 7244–7249. (d) Lim, C.-H.; Ryan, M. D.; McCarthy, B. G.; Theriot, J. C.; Sartor, S. M.; Damrauer, N. H.; Musgrave, C. B.; Miyake, G. M. *J. Am. Chem. Soc.* **2017**, *139*, 348–355. (e) Treat, N. J.; Sprafke, H.; Kramer, J. W.; Clark, P. G.; Barton, B. E.; Read de Alaniz, J.; Fors, B. P.; Hawker, C. J. *J. Am. Chem. Soc.* **2014**, *136*, 16096–16101.

(18) Gottlieb, H. E.; Kotlyar, V.; Nudelman, A. *J. Org. Chem.* **1997**, *62*, 7512–7515.

(19) *Gaussian 09*, Revision A.02: Frisch, M. J.; Trucks, G. W.; Schlegel, H. B.; Scuseria, G. E.; Robb, M. A.; Cheeseman, J. R.; Scalmani, G.; Barone, V.; Mennucci, B.; Petersson, G. A.; Nakatsuji, H.; Caricato, M.; Li, X.; Hratchian, H. P.; Izmaylov, A. F.; Bloino, J.; Zheng, G.; Sonnenberg, J. L.; Hada, M.; Ehara, M.; Toyota, K.; Fukuda, R.; Hasegawa, J.; Ishida, M.; Nakajima, T.; Honda, Y.; Kitao, O.; Nakai, H.; Vreven, T.; Montgomery, J. A., Jr.; Peralta, J. E.; Ogliaro, F.; Bearpark, M.; Heyd, J. J.; Brothers, E.; Kudin, K. N.; Staroverov, V. N.; Kobayashi, R.; Normand, J.; Raghavachari, K.; Rendell, A.; Burant, J. C.; Iyengar, S. S.; Tomasi, J.; Cossi, M.; Rega, N.; Millam, J. M.; Klene, M.; Knox, J. E.; Cross, J. B.; Bakken, V.; Adamo, C.; Jaramillo, J.; Gomperts, R.; Stratmann, R. E.; Yazyev, O.; Austin, A. J.; Cammi, R.; Pomelli, C.; Ochterski, J. W.; Martin, R. L.; Morokuma, K.; Zakrzewski, V. G.; Voth, G. A.; Salvador, P.; Dannenberg, J. J.; Dapprich, S.; Daniels, A. D.; Farkas, Ö.; Foresman, J. B.; Ortiz, J. V.; Cioslowski, J.; Fox, D. J. *Gaussian, Inc.*: Wallingford, CT, 2009.

(20) *Spartan'14*; Wavefunction, Inc.: Irvine, CA, 2014.

(21) (a) Zhang, S.; Liu, X.; Wang, T. *Adv. Synth. Catal.* **2011**, *353*, 1463–1466. (b) Schmidt, R.; Thorwirth, R.; Szuppa, T.; Stolle, A.; Ondruschka, B.; Hopf, H. *Chem. - Eur. J.* **2011**, *17*, 8129–8138.

(22) Li, L.; Rosenthal, M.; Zhang, H.; Hernandez, J. J.; Drechsler, M.; Phan, K. H.; Rütten, S.; Zhu, X.; Ivanov, D. A.; Möller, M. *Angew. Chem., Int. Ed.* **2012**, *51*, 11616–11619.